PLASMA-WALL-INTERACTION: IMPORTANT ION INDUCED SURFACE PROCESSES AND STRATEGY OF THE EU TASK FORCE

Joachim Roth[1], *Emmanuelle Tsitrone*[2], *Alberto Loarte*[3]

[1] Max-Planck-Institut für Plasmaphysik, EURATOM-Association, 85748 Garching, Germany
[2] Association Euratom-CEA, CEA/DMS/DRFC CEA Cadarache, 13108 Saint Paul lez Durance, France
[3] EFDA-Close Support Unit Garching, 85748 Garching, Germany

Abstract:

In future thermo-nuclear fusion devices, such as ITER (International Thermonuclear Experimental Reactor), the interaction of the plasma with surrounding materials in the vacuum vessel constitutes one of the main remaining engineering problems. The choice of materials is a crucial point, which will determine issues such as the plasma facing components lifetime before refurbishment or the tritium inventory build up in the vessel, which should be limited for safety reasons. In order to tackle these issues, the European Task Force on Plasma wall interaction has been implemented in the frame of EFDA (European Fusion Agreement) in the fall 2002 with the aim "to provide ITER with information concerning lifetime-expectations of the divertor target plates and tritium inventory build-up rates in the foreseen starting configuration and to suggest improvements, including material changes, which could be implemented at an appropriate stage."

The EU PWI TF brings together the efforts of 24 European associations in the following fields of investigation :

- Material erosion and transport in tokamaks
- Tritium inventory and removal
- Transient heat loads on plasma facing components
- Dust production and removal
- Associated modelling and diagnostic development

This paper will present the organisation of the EU PWI TF. It will provide examples for the multitude of surface processes in plasma-wall interaction and present the status of knowledge concerning material erosion and hydrogen retention for the choice of ITER materials (Beryllium, Carbon and Tungsten).

I. Introduction:

ITER (International Thermonuclear Experimental Reactor) is a joint international research and development project that aims to demonstrate the scientific and technical feasibility of fusion power. The partners involved in the project are the European Union (represented by EURATOM), Japan, the People´s Republic of China, India, the Republic of Korea, the Russian Federation and the USA. In May 2006, the partners met to sign an agreement on the joint implementation of ITER construction, operation, and decommissioning. ITER will be constructed in Europe, close to the research centre of Cadarache in the South of France.

The collaborative result of decades of fusion research on the energy production in the fusion reaction D+T->He+n from many magnetic fusion devices world-wide has resulted in a design which meets the following scientific and technological objectives :

- a long-pulse (~8 min) burning fusion plasma at an energy amplification factor, *Q*, of at least 10 ($Q = P_{fusion}/P_{heating}$ is the ratio of power produced by fusion reactions versus the power required to heat up the plasma by external means),
- the capability to investigate steady-state plasma operation at lower Q, ($Q = 5$) with pulse lengths of the order of 30 min,
- integration and investigation of fusion technology relevant for the first commercial-type fusion reactor (DEMO).

However, questions remain open, in particular in the field of plasma wall interactions. Indeed, in comparison with present day devices, ITER represents a major step forward in terms of plasma wall interactions, namely due to the increase in the plasma energy and extended duty cycle. While the size of ITER is about two times larger than the largest present experiment, JET, the stored energy in the plasma is a factor of 35 and the ion fluences per discharge a factor of 1000

higher. Integrated scenarios for power and particle exhaust have been developed, based on high-density plasma operation in front of the most power loaded areas of the vacuum vessel (divertor plates, see fig. 1), which leads to plasma detachment (regimes at low electronic temperature, T_e ~ few eV), reducing the peak divertor power loads by atomic processes such as radiation, charge exchange and recombination (see section III-1). However, even in these regimes, the constraints on the plasma facing components (PFCs) remain severe :

- to ensure heat exhaust at significant power loads (up to 10MWm^{-2} to extract continuously on the divertor target plates), as well as handling of higher transient heat loads. In any case excessive sublimation or melting of the target materials must be avoided.
- to achieve sufficient lifetime of the plasma-facing components (>3000 ITER full performance shots). This goal is largely related to the control of transient heat loads due to events such as edge localized modes (ELMs), which are fast repetitive heat and particle expulsions from the plasma occurring during the high performance scenario foreseen for ITER, and disruptions, which is a loss of control of the plasma resulting in a fast energy peak on PFCs.
- to ensure the He ash exhaust and an acceptable level of contamination of the plasma by the material eroded from the walls.
- to stay below the long-term tritium (T) vessel inventory limit, which is set by safety considerations to 350 g of T.

In the issues listed above, the most critical ones are the PFCs lifetime and the T retention in the vessel. Indeed, extrapolation from present day devices shows that ELMs and disruptions can strongly limit the PFCs lifetime [1]. Work is ongoing to design scenarios with tolerable ELMs and to mitigate disruptions. In the same way, extrapolation from present day devices with all carbon walls show that the T inventory limit could be reached within less than 100 full performance discharges [2]. Indeed, the main retention processes identified so far are linked to

carbon erosion, transport and re-deposition, leading to fuel trapping in the re-deposited layers [3]. The material mix foreseen for ITER (Beryllium (Be) for the first wall (700 m^2), Tungsten (W) on the upper divertor regions and the dome (100 m^2), carbon (C) on the divertor plate (50 m^2), see figure 1) should therefore reduce this constraint compared with full carbon machines. However, predicting PFCs lifetime and T retention under these conditions remains challenging (see section V). Experiments are starting in European fusion devices to test these material combination : full W machine in ASDEX Upgrade (Germany) [4], Be first wall and W divertor in JET (European facility located in England) [5]. Techniques to mitigate the T retention and to remove T from the PFCs are also under development. Finally, if the T retention remains unacceptably high with the C targets, a full tungsten device could be contemplated in a second phase.

Gelöscht: metal

In this context, a coordinated European research activity has been established (EU Task Force on Plasma–Wall Interaction) with the aim "to provide ITER with information concerning lifetime-expectations of the divertor target plates and tritium inventory build-up rates in the foreseen starting configuration and to suggest improvements, including material changes, which could be implemented at an appropriate stage.". The purpose of this contribution is to outline the strategy of the EU-PWI-TF and demonstrate needs for basic PWI research. To illustrate this point, it will focus in the second part on the issue of controlling the tritium inventory in ITER.

II Strategy and organisational structure of the EU Task Force on Plasma-Wall Interaction

Gelöscht: of the

After installation of the EU-PWI-TF in 2002, each EU association was asked to nominate a contact person for the TF to coordinate the EU PWI work within the association, to transfer the knowledge from the association to the TF and vice versa and to participate actively on the TF meetings. The role of the contact persons in the EU TF structure is essential for a successful TF work

High priority issues have been identified and special expert working groups (SEWGs) have been set up to work on well defined subtopics (see list of issues and SEWGs in table 1, for more details, see the TF website www.efda-taskforce-pwi.org). SEWGs define coordinated experiments to be performed in fusion devices, plasma simulators or ion beam experiment, and gather the associated results for comparison. Meetings at the working level and exchange of scientists to participate in collaborative experiments is encouraged through mobility funding by EFDA. New SEWGs can be created if needed, or ended after completion of the related work.

A 3 years work programme has been established from the commitments of each association in the various working areas. This work programme, based on the voluntary contributions of the associations, is periodically reviewed and can be found on www.efda-taskforce-pwi.org under "Work Programme".

Finally, in close consultation between the task force leaders and SEWG leaders, technology tasks partially funded by EFDA (up to 40% in the present organisation) can be issued on urgent topics not covered adequately in the voluntary program of the associations. These tasks have well defined deliverables, deadlines (typically 1 year duration) and budget. New tasks are sent to all Heads of associations and TF contact persons to ensure widespread information and contributions. Final progress reports are being made available on the EU TF web page. As an example, the list of tasks issued in 2006 are introduced in table 1.

A general TF meeting is organised once a year, where progress in the SEWGs, status of the EFDA technology tasks and reports from the associations are presented. Latest news on the ITER design and orientations for future work (new SEWGs etc) are also discussed (see on www.efda-taskforce-pwi.org under "Meetings" to view presentations shown at the last meetings).

The general work of the EU PWI TF has also been presented in several publications (e.g. [6]).

III. Tritium retention in tokamaks

One of the most important ongoing tasks is to evaluate, in view of the experiences of the present (mostly full) carbon-clad fusion devices, the implications of the use of graphite at the lower target area in ITER with respect to **long term tritium retention.** The question of the target lifetime has a lower critical priority for ITER (not for a future power plant), as calculated margins seem acceptable [1] provided scenario with tolerable ELMs are developed.

Present tokamak experiences show clearly that the majority of the long term tritium retention is due to co-deposition of tritium along with eroded carbon forming tritium-rich carbon co-deposits. For extrapolation of the inventory observed in present fusion experiments, where most plasma-facing components are made from carbon materials, to the next step device, ITER, a fundamental understanding of the different steps involved in the co-deposition process is necessary :

- implantation of energetic particles into the wall material
- erosion of wall material
- transport of the eroded material within the plasma
- re-deposition, sticking and re-erosion
- co-deposition of fuel with the eroded material

The goal is to identify the important parameters that determine these processes, such as the divertor geometry, the divertor and edge plasma conditions, the wall surface temperature, in order to propose possible operational and design improvements for ITER.

III-1) Parameters of the plasma in contact with plasma facing components in ITER [7]

Because of the large plasma densities in the confined plasma (~ 10^{20} m^{-3}) required for fusion energy production in ITER [8] and the resulting large power outflow from the confined plasma, the energy fluxes and plasma parameters in contact with ITER plasma facing

components will span a range far beyond that achievable in present fusion devices. For the reference ITER operation regime with a fusion power gain Q = 10, the expected power flow from the main plasma onto the plasma facing components is ~ 100 MW. Due to the magnetic configuration of the tokamak, the power carried by the charged particles of the plasma can be concentrated on a narrow area around the strike points on the specially designed divertor target plates (see figure 1). In the absence of any dissipative power loss in the plasma periphery, such a power flow would lead to a peak power flux at the strike points ~ 30 MWm^{-2}. From the technology point of view, this is a factor 3 larger than what can reliably be achieved for water-cooled plasma facing components [9].

Therefore scenarios with enhanced dissipative power losses in the plasma boundary have been developed, yielding low plasma temperatures (~ 5 eV and lower). This allows to access to the detached divertor regime [10], which is the reference for ITER divertor operation [11]. In the detached divertor regime, dissipation of the power conducted/convected by the plasma by the high densities due to intense hydrogen recycling, impurities radiation, and partial recombination of the impinging particle flux allows to keep peak power fluxes on the divertor targets under ~ 10 MWm^{-2}, while maintaining adequate central plasma purity [11]. The corresponding ITER plasma parameters along the divertor target estimated from modelling are shown in Fig. 2 [11, 12].

Near the plasma strike point the typical plasma/neutral fluxes reach values larger than 10^{24} $m^{-2}s^{-1}$ (leading to a total fluence > 10^{26} m^{-2} for each ITER pulse) with plasma densities in the order of ~10^{21} m^{-3} and plasma temperatures of ~ 3 eV. This corresponds to an ion impact energy of ~15 eV, due to acceleration by the plasma sheath potential. Despite these low impact energies, the power flux deposited on the water cooled ITER divertor target is significant, leading to an expected surface temperature of ~ 1500 K around the strike points [12]. The interaction of such high density/low temperature plasma with material surfaces at high temperatures could never be

investigated in fusion research devices (neither the power fluxes nor the plasma densities are accessible to present devices) and may lead to qualitative changes in the processes that govern this interaction with respect to today's experiments [13].

In contrast with the divertor, the present physics understanding of particle fluxes, plasma densities and temperatures in contact with the first wall of ITER is more uncertain (ITER PFCs geometry is shown in Fig. 3.a [14]). Present modelling results indicate that the flux of neutrals, produced by charge-exchange processes between the incoming cold recycling D/T neutrals and the hot edge plasma, is in the range of 10^{19}-10^{21} $m^{-2}s^{-1}$ with typical energies ~ 8 – 300 eV, as shown in Fig. 3.b [14]. The flux maxima observed correspond to sources of neutral atoms which undergo charge-exchange collisions with hot plasma ions, such as the gas injection at the top of the machine (~8m on the x axis), or recycling from the inner (~0m) and the outer (~18m) divertor plate. They are associated with a decrease in the mean energy, due to the contribution of the cold recycling neutrals from the source. The energy of the neutrals hitting the wall peaks at the plasma edge temperatures, but has contributions up the central plasma temperature [15].

Gelöscht: ,

In a tokamak, particle and energy transport are much faster along than across the magnetic field, leading to a concentrated interaction between the plasma and the wall in the regions where the magnetic field lines are first intercepted (such as the divertor strike points, located on the first magnetic surface intercepting an object, called separatrix). When going away from this region, the particle and heat flux are expected to decrease rapidly (with a typical decay length of ~1 to a few cm, as shown in figure 2 on the divertor targets).

From this, a moderate plasma flux should impact the first wall of ITER, located several cms away from the separatrix. However, recent results have shown that the plasma fluxes on the wall can be higher than expected from this simple exponential decay, due to turbulent transport across the field lines [16]. Present modelling [11, 17] assumes the integrated plasma flux on the ITER

wall to be in the range of 10^{23}-10^{24} s^{-1}, which leads to an average flux on the Be wall (~ 700 m^2) of 1.4 10^{20} – 1.4 10^{21} $m^{-2}s^{-1}$. Associated typical plasma temperatures are in the range of 10-20 eV, leading to ion impact energies of 50 - 100 eV.

III-2) Observations on fuel retention in present devices

The retention of hydrogen in graphite by implantation and the formation of amorphous hydrogen-rich carbon layers upon impact of carbon atoms or ions together with hydrogen species has been well known since long and has also been observed in fusion devices [1,18,19], although it was not an operational problem for machines operating in pure deuterium plasma.

However, the severity of the problem for the next-step device became strongly evidenced after first tritium experiments in TFTR [20] and JET [21]. About 3 and 36 g of T were injected in TFTR and JET respectively, from which large amounts (30–40%) were retained in the machine at the end of the T campaign (a few days), as shown in figure 4 upper part. Large amounts of fuel are also observed to be retained in the wall at the end of single discharges, e.g. in JET, Tore Supra [22] and other machines (e.g. [2,19]). Results from long pulse machines such as Tore Supra show that with actively cooled PFCs, the wall does not saturate but maintains a constant retention rate all along the discharge ([23]). Despite the application of various cleaning methods [1] (not discussed here), about 13% and 10% of the T remained in TFTR and JET [24], respectively. These observations are well in line with findings for long term retention in devices operating in deuterium, such as TEXTOR (8%) [25] or ASDEX Upgrade (3%) [26]. Extrapolating such values (long term retention fraction ~ 10% of the injected fuel) to ITER (fuelling rate 200 Pam^3 s^{-1} of half D/T mixture) the T safety limit of 350 g would be reached in less than 50 full performance 400 s plasma discharges. Thereafter, cleaning procedures must be applied to recover the fuel before further tritium plasma operation. It has to be noted that this

long term retention fraction of 10 % is derived from carbon dominated machines, and the material mix foreseen for ITER could largely relax these numbers. Recent experiments in ASDEX Upgrade, replacing progressively its C PFCs by W, have shown a reduction of the carbon concentration by 70% while the main carbon source are the divertor plates [27]. Experiments with a full W machine are planned for 2007.

It is found that the majority of the long-term retained fuel is stored in carbon layers built up by re-deposition of eroded carbon along with the hydrogenic fuel (co-deposits) formed at remote locations in the machine [25,28,29,30]. On erosion-dominated graphite areas, the fuel retention is restricted to implantation in a shallow surface layer, enhanced by porosity, e.g. due to adsorption onto inner surfaces of CFC tiles, saturating at few 10^{17} H/cm^2 [8,31]. This would extrapolate to ~5 g T for the total wall area of ITER (if one assumes it is covered by carbon) and is tolerable.

Gelöscht: 24

Co-deposited C- layers, however, contain hydrogen fractions up to H/C=1, depending on the surface temperature and impact particle energy. This process does not saturate and is continuous, with the deposited layer growing as long as erosion occurs. Layers are formed preferentially in places not loaded with intense plasma fluxes, but also on areas with no direct plasma ion impact (‘remote areas’, such as gaps between tiles, entrance to pumping ducts). This can be seen on figure 4, lower part, where the T inventory in units of TBq found from post mortem analysis of JET tiles after the first full D/T campaign is shown. Moderate amounts of T are found in the erosion dominated outer divertor, while higher T content is found in deposition areas in the inner divertor. However, the strongest concentration of T was found in deposits and flakes on the inner divertor louvers (circled in figure 4) at the entrance of the pumping ducts.

As was shown in this section, the plasma parameters, discharge duration as well as the PFC materials and temperature will significantly differ in ITER compared to present day devices.

Therefore, extrapolating to predict T retention or PFC lifetime requires a detailed understanding of the underlying PWI processes. The next section will describe the present status of knowledge.

IV Investigation of PWI processes for retention in fusion relevant materials

IV-1) Implantation

Implantation of low-energy hydrogen ions into materials, such as carbon [32,33], tungsten [34] and beryllium [35,36], has been investigated in detail and ion ranges and hydrogen retention profiles have been compared to Monte Carlo code calculations. The distributions are typically well reproduced and the underlying physics in electronic and nuclear stopping is well understood.

For carbon, the situation is not so clear. Indeed, in pyrolytic graphite or fine grain graphites with low porosity, hydrogen does not diffuse and after reaching a local concentration in the implantation range of D/C= 0.4 further hydrogen is reemitted as expected [37]. However, in more porous materials [38], like carbon fibre composite (CFC) materials [39] contemplated for ITER due to their good thermo-mechanical properties, the behaviour is different. To investigate this point, recent coordinated experiments have been performed at high fluence in ion beams, plasma devices and tokamaks. Results have shown no saturation of the total implanted amount as a function of fluence. Instead, the retained amount increases as the square root of the ion fluence (see fig. 5) due to diffusion deep into the bulk. This inward diffusion shows a very low activation energy and details of the transport process are poorly understood [39]. This could have implication for long pulse/high fluence machines such as ITER, and probably plays a role to explain the retention rate observed in the long pulses of Tore Supra [23].

Gelöscht: 27

In many metals, including Be and W, deuterium is highly mobile and is only retained in radiation damage or defects of the crystal lattice [40,41]. After saturating available traps in the ion induced damage profile, inward diffusion and subsequent trapping at lattice defects increases

the total amount similarly to the case of porous graphites and the resulting retention depends critically on the crystallinity of the substrate. The retention increases from single crystals, to well annealed polycrystalline material and high values in plasma-sprayed W coatings [42]. As the build-up of the inventory is diffusion limited, it increases only with a square-root dependence on the fluence and stays tolerable at high fluences (fig. 5). While at ion fluences typical for today's fusion devices of the order of 10^{24} D/m^2 and discharge, only a fraction of 10^{-3} of the incident fluence is retained, this fraction levels off to negligible values for ITER fluences expected to exceed 10^{26} /m^2 and discharge. Similar behaviour is observed for Be [36], although the database is much less broad.

Gelöscht: 24

IV-2) Codeposition

IV-2-a) Erosion of plasma facing materials

The first step in the chain of processes leading to fuel inventory build-up by co-deposition is the erosion of the wall material. In the keV energy range **physical sputtering** of solids is well described by theory [43], while in the range below 1 keV, especially for light ions, threshold effects have to be considered [44,45]. A broad experimental data base exists today and even down to yields of the order of 10^{-5} the data are well reproduced by Monte Carlo codes simulations, such as SPTRIM [46] (fig. 6). In view of uncertainties in the edge and divertor plasma parameters in future fusion devices, the precision of the sputtering yield data is very good for wall lifetime and tritium inventory estimates.

The situation is different for carbon based materials. In this case the chemical interaction with the hydrogen plasma leads to enhanced **chemical erosion** yields [47] (fig. 6). Chemical erosion is a complicated, multi-step process which was discovered in 1976, and still exhibits many unresolved details. It will be reviewed in this volume by F. Meyer [48] and cannot be reproduced here in detail. The main features, important for the co-deposition chain are:

- Enhanced yields at elevated temperatures with a maximum around 600-800 K and yields around 10^{-1}.
- Emission of hydrocarbon molecules and radicals with different sticking behaviour on surfaces.
- At least two erosion processes are involved: a thermal reaction process (no threshold, no isotope effect) [49] and a kinematical process at room temperature and low ion energies (energy threshold observed in plasmas [50] and MD calculation [51]).
- A flux dependence becoming obvious at fluxes above 10^{22} D/m^{2}s and decreasing the chemical erosion yield to values well below 10^{-2} [52].

After cross examination and recalibration of data from different experimental devices within EU, the large experimental data base could be unified, an analytic description [52] including the flux dependence could be developed for extrapolations to ITER edge plasma and divertor conditions. Critical, and insufficiently known parameters are the threshold behaviour [53], the contribution of heavier hydrocarbons and radicals [54], the influence of the chemical reactivity due to simultaneously incident energetic impurity ions [55,56] and the origin of the flux dependence.

IV-2-b) Re-deposition of hydrocarbon radicals

The emitted molecules will enter the plasma, get ionised and partially dissociated and will be transported along magnetic field lines to wall surfaces. Important for the estimate of tritium inventory is the sticking probability to the surface and, consequently, the re-emitted or re-eroded fraction which may escape the divertor plasma and be co-deposited with tritium in remote areas of the vacuum vessel. While the inventory in deposited layers on the divertor target is small due to the high surface temperatures of 800 to 1700 K [12], the hydrogen isotope concentration in remote layers at lower temperature can reach D,T/C values of 1.

The sticking coefficient depends strongly on the kind of hydrocarbon molecules and the deposition conditions. An example is shown in fig. 7 for the case of CH_3 incident in Si surfaces. For a CH_3 particle beam alone the sticking coefficient on a typical hydrogen saturated layer is of the order of 10^{-4}, while simultaneous bombardment by incident hydrogen ions provide bonding sites for CH_3 by hydrogen removal, such that the sticking coefficient increases into the 10^{-2} range [57].

Gelöscht: (fig. 7)

A collection of sticking coefficients for different hydrocarbon molecules measured experimentally [58] and calculated using molecular dynamics (MD) codes as function of incident ion energy [59] is given in table 2.

At thermal energies the sticking coefficient depends strongly on the electronic configuration of the hydrocarbon molecules. While at thermal energies there is reasonable agreement of experimental data and MD calculations, the calculations predict sticking coefficients close to unity at energies above 10 eV.

Detailed information can only be provided by dedicated lab experiments. For instance, the energy dependence of the re-emitted ion flux was determined [60] as a function of internal energy of the molecules. While without excitation decomposition of incident CH_4^+ molecules starts only at 30 eV, indicating that the whole dissociation energy must be supplied by the surface collision, for high internal excitation sufficient to provide the decomposition energy of 1.8 eV the reemission of CH_4^+ decreases monotonically with ion energy. Data for sticking coefficients on realistic plasma-facing materials were presented in this conference [61].

Gelöscht: will be

IV-2-c) Re-erosion by the hydrogen plasma

A major effect in the final deposition of hydrocarbons is their re-erosion by the impact of plasma ions and atomic hydrogen. Modelling of erosion/redeposition balance indicates that re-deposited hydrocarbon layers in tokamaks are subject to an "enhanced" chemical erosion with yields in the range of ~ 10 % under plasma impact [62]. This is in agreement with laboratory

Formatiert: Nicht Hochgestellt/ Tiefgestellt

experiments of the chemical erosion of (soft, hydrogen-rich) a-C:H layers showing much higher erosion yields by thermal atomic hydrogen when compared to graphite [63]. The rate for re-erosion of a-C:H layers by atomic hydrogen is temperature dependent as demonstrated in experiments in the PSI-2 simulator, while hydrocarbon deposition is not [64]. Thus, it is generally found that the combination of all the complex processes involved in the final deposition of hydrocarbons is such that there is a prevalence of hydrocarbon deposition at low surface temperatures and of erosion at high temperatures, as shown in Fig. 8 for experiments performed at the PSI-2 plasma simulator [65].

Formatiert: Nicht Hochgestellt/ Tiefgestellt

Formatiert: Nicht Hochgestellt/ Tiefgestellt

Formatiert: Nicht Hochgestellt/ Tiefgestellt

However, the temperature at which this balance shifts from deposition to erosion seems to be different in the various experiments, as expected from such a complex balance of processes. For example, studies with temperature controlled samples exposed in the private flux region of the divertor in ASDEX Upgrade show that carbon deposition can be reduced by about one order of magnitude by increasing the temperature from 50 to 100^{o}C and by a further factor of 3 when going from 100 to 200^{o}C, but complete suppression of re-deposition cannot be achieved within this temperature range [66]. This is in qualitative agreement with the experimental results in PSI-2, but the temperature of transition from deposition to net erosion depends strongly on the respective ration of hydrocarbon to atomic hydrogen flux.

Formatiert: Nicht Hochgestellt/ Tiefgestellt

IV-2-d) Co-deposition of hydrogen atoms

The final step in the co-deposition process is the incorporation of hydrogen upon deposition in remote areas, not seen by the plasma for further re-erosion. Impurity atoms or molecules are deposited together with a flux of energetic or thermal neutral hydrogen atoms. For carbon deposition, amorphous hydrogenated carbon(a-C:H) layers are formed, where the hydrogen concentration and the hardness of the layer depend critically on the energy of the simultaneously incident flux of hydrogen. Energetic ions lead to the deposition of hard films with hydrogen concentrations H/C of about 0.4, while low energy thermal hydrogen leads to the formation of soft films, with H/C concentrations exceeding 1 [67,68]. In fig. 9 the amount of retained hydrogen in deposited films of C, Be and W is shown on collectors mounted in front of targets irradiated with 1 keV D ions [69]. Thus, together with the deposited sputtered atoms, a flux of reflected energetic deuterium atoms hits the collector. Under these conditions the carbon film contains 0.41 D/C. In contrast to carbon, for deposited metals a very low retention is expected due to the fast out-diffusion of hydrogen. This is indeed the case for W, while for Be the

oxidation of the layer to BeO is responsible for a deuterium uptake which can be similar to carbon..

The data of fig. 9 were obtained from collectors at room temperature. The concentration in the deposited films is strongly dependent on surface temperature. Especially for metals and BeO the concentration decreases strongly already above 500 K [70]. For carbon the concentration decreases only at more elevated temperatures, and values on D/C between 1 in remote areas and 0.01 on high heat carrying surfaces are measured in fusion devices [71,72,73].

The hydrogen concentration in deposited films, with its dependence on plasma conditions, geometry towards the eroded surfaces, impurity content and temperature, still is one of the largest uncertainties in the estimate of tritium inventory in ITER.

V Present estimate for ITER inventory

Based on the present status of knowledge, attempts were made to estimate the T inventory in ITER as function of shots with the following inputs :

- plasma conditions expected from plasma codes [11]
- erosion yields dependent on energy, temperature and ion flux
- transport of hydrocarbon molecules in the plasma boundary,
- deposition with sticking coefficients between 0 and 0.5 for hydrocarbons
- re-erosion from the divertor plate with enhanced yield for thermal hydrogen atoms
- Concentration of T of 30 % in co-deposition layers from carbon atoms which escape re-deposition at the divertor plate

Results are summarised in fig. 10.

As already mentioned, a simple scaling, based on a long term retention fraction of 10% of the injected fuel obtained in today's all carbon devices, e.g. JET, leads to a very limited number of discharges (< 50) before reaching the safety limit (350 g T). First calculations by Brooks et al

[74] predicted reaching the safety limit in more than 100 discharges taking into account that only the divertor plates will be made from carbon materials (see Brooks 2003 on figure 11). In their analysis, a constant chemical erosion yield of 0.015 was assumed, neglecting the dependence on surface temperature, energy and ion flux. Taking these dependencies into account, Roth et al. [75] arrived at more relaxed conditions predicting an operation period of 600 to 1500 discharges to reach the limit (see Roth 2004 on figure 11), with the sticking coefficient at the divertor plates being the largest source of uncertainty. In the calculations, the range of the retention per discharge is due to different sticking coefficients assumed for hydrocarbon molecules and radicals at the divertor plate, varied between 0 and 0.5, while coefficients for the sticking of carbon atoms are taken from MD calculations. More recently, Kirschner et al. [76] tried to take into account a possible enhanced re-erosion of the deposit at the divertor plate ($10xY_{chem}$), and the effect of Be being eroded at the main vessel surface and co-deposited on the divertor plate. Although the Be reduces the chemical re-erosion of carbon, it strongly enhances the retention assuming a D/Be ratio of 0.05, reducing the operation time to about 150 discharges. For Be concentrations in the plasma over 1 %, carbon is not eroded any more due to Be layer build-up and tritium retention gets dominated by co-deposition with Be. In this evaluation the Be concentration in the incident plasma, the re-erosion of the layers and, again, the sticking coefficient of hydrocarbon molecules are the dominant uncertainties. It has to be noted that tools for modelling material erosion and co-deposition, such as the ERO code [77] used to derive results shown on figure 11, are being developed with the support of the EU PWI TF.

Gelöscht: .

While further research may improve the precision of the predictions, it seems clear that with the use of carbon as divertor material, mainly motivated by handling transient heat loads without melting, the T safety limit will be reached within a few tens-hundreds discharges, after which operation has to stop for the vessel to be cleaned and tritium to be recovered. Cleaning methods

have to be developed and tested under realistic fusion conditions. In any case, it is recommended that the machine design allows enough flexibility to ultimately change the divertor as well as the first wall PFCs material.

VI. Summary

As ITER is being started in 2006, plasma-wall interaction processes are critically defining the plasma-facing material choice. The main issue is the accumulation of a tritium inventory exceeding the safety limit. For improving understanding and credible extrapolations further basic research is necessary on several individual steps in the tritium retention chain:

- implantation, diffusion and retention in ITER relevant materials
- Erosion, impurity transport and re-deposition on vessel walls
- Co-deposition of hydrogen isotopes in form of hydrogenated layers

The EU PWI TF concentrates the knowledge of 24 European associations on these problems. The tools are the voluntary work programme agreed by the associations, concentrated in SEWGs on very urgent, critical topics. Additionally, research is supported and steered by a relatively small technology programme with financial support for well defined tasks.

Table 1: Priority issues listed by the EU PWI Task Force, associated Special Expert Working Groups and EFDA technology Tasks issued in 2006

Topics	SEWGs	EFDA Technology Tasks
Material erosion and transport in tokamaks	Erosion and transport of carbon	- Reflection properties of hydrocarbon radicals for ITER divertor conditions - Erosion/re-deposition balance in ITER-relevant divertor tokamaks - Material erosion and re-deposition in ITER relevant divertor target temperatures, plasma impact energies and divertor chamber conditions
	High Z materials	- Fuel retention in metallic materials for ITER. - Coating of EU CFC/W targets with beryllium for experiments in Russian plasma guns
	ITER like material mix	- Improvement of the ERO code for advanced description of mixed material formation in ITER reference scenarios - Molecular dynamics simulations of mixed material formation at the ITER divertor
Fuel retention and removal	Gas balance and fuel retention	-Tritium retention in ITER relevant mixed-materials
	T removal	-Tritium removal from macro-brush structures by oxidative methods
Transient heat loads and control	Transient heat loads	- Modelling of ITER plasma-facing component damage following ELMs and disruptions - Material damage for CFC and W under large cycle under-threshold ITER ELM-like loads simulated with an e-beam - Analysis of be-coated and be-clad targets exposed to Russian plasma guns
Dust production and removal	Dust in fusion devices	- Evaluation of dust generation mechanisms at the ITER SOL and divertor plasma
PWI modelling		- Modelling of far SOL plasma profiles in ITER reference scenarios for optimisation of ICRH coupling calculations. - Self-consistent modelling of plasma-wall interactions and SOL transport with real 3-D plasma facing component geometries for ITER reference scenarios - Modelling of erosion/re-deposition for ITER limiter ramp up/down and reference scenarios including macro-brush & gap geometries, temperatures and surface composition
Task force relevant diagnostics		- Diagnostic techniques for time resolved dust measurement in tokamaks

Table 2: Sticking coefficients for hydrocarbon molecules and radicals from experiments (left column) and molecular dynamics simulation (right column)

Sticking Coeff.	Experimental for 1100 K	MD simulations for 0.02 to 10eV
CH_4	0	n.a.
CH_3	10^{-4} to 10^{-2}	0.02 to 1
CH_2	0.025	0.03 to 1
CH	1.	n.a
C	1	1
C_2H	0.8	0.15 to 1
C_2H_3	0.35	0.02 to 1
C_2H_5	0.03	n.a.

Figure Captions:

Figure 1. Cut-away showing the layout of PFCs in ITER with different armour materials. The divertor target plates shown in red are made of carbon, the upper baffles and the dome shown in green are made of tungsten, while the first wall shown in blue is made of beryllium. Magnetic surfaces are also shown.

Gelöscht: e

Figure 2. Plasma temperature T_e, density n_e, D/T ions and neutrals particle fluxes, heat fluxes and surface temperature along the ITER outer divertor target for a semi-detached divertor plasma for the ITER =10 reference scenario. x = 0 on the x axis corresponds to the strike point position, x < 0 corresponds to the region located below the strike point, x > 0 corresponds to the region located above the strike point.

Figure 3.a. ITER poloidal cross-section showing inner (IW) and outer (OW) first wall, divertor vertical target (VT), divertor baffle (B) and divertor private region consisting of dome (D) and liner (L). Scrape-off-layer surfaces including the separatrix are shown; the numbers along the cross section give poloidal distances in meters along the separatrix, which are used in Fig. 3.b
Figure 3.b. Modelled charge-exchange neutral flux and average neutral impact energy on the ITER Be first wall versus poloidal distance as defined in Fig.3.a.

Figure 4. Upper: cumulative retention of tritium inside JET and TFTR after the tritium plasma operation campaigns [20,21]. Lower: tritium distribution in the JET tiles after cleaning procedures measured by post mortem surface analysis [24].

Figure 5. Retention of 200 eV D^+ deuterium in carbon (pyrolytic graphite and CFC) and polycrystalline tungsten

Figure 6. Sputtering yield of Be, C and W due to deuterium ions compared to an analytic description of physical sputtering.

Figure 7. Growth rate of a layer on Si due to CH_3 exposure at constant flux of $5*10^{14}$ $cm^{-2}s^{-1}$ as function of simultaneous bombardment by incident hydrogen flux

Figure 8. Balance of erosion and deposition at the plasma edge and pump duct in the PSI-2 plasma simulator versus sample temperature [65].

Figure 9. Co-deposited amounts of deuterium on a collector in front of different samples sputtered by 1 keV D^+ ions

Figure 10. Estimated tritium inventory as function of the number of full, 400 s ITER D/T discharges. For details, see text.

Figure 1. Cut-away showing the layout of PFCs in ITER with different armour materials. The divertor target plates shown in red are made of carbon, the upper baffles and the dome shown in green are made of tungsten, while the first wall shown in blue is made of beryllium. Magnetic surfaces are also shown.

Gelöscht: ev

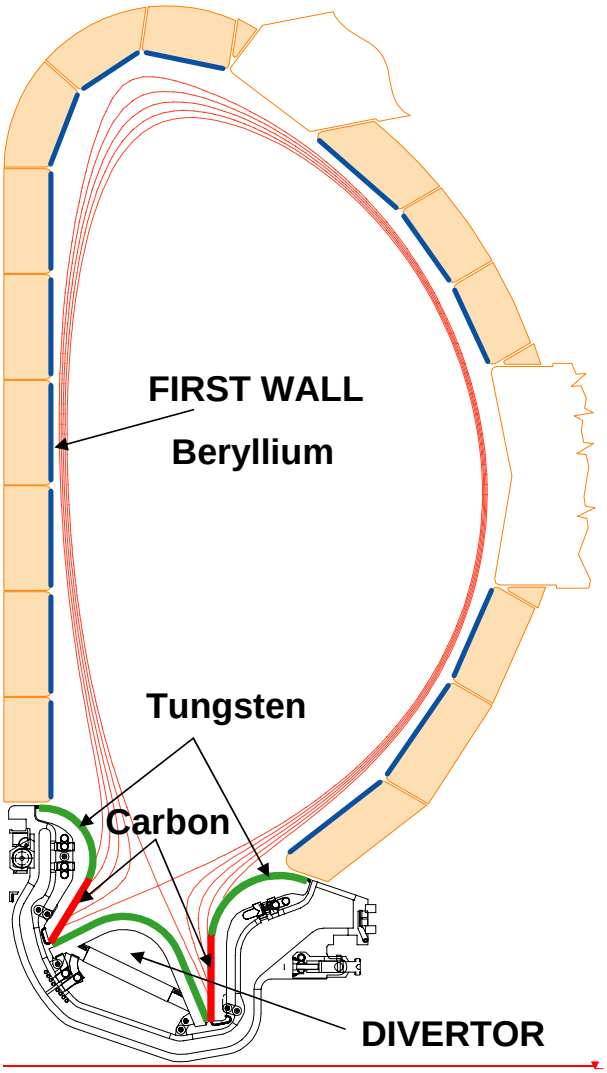

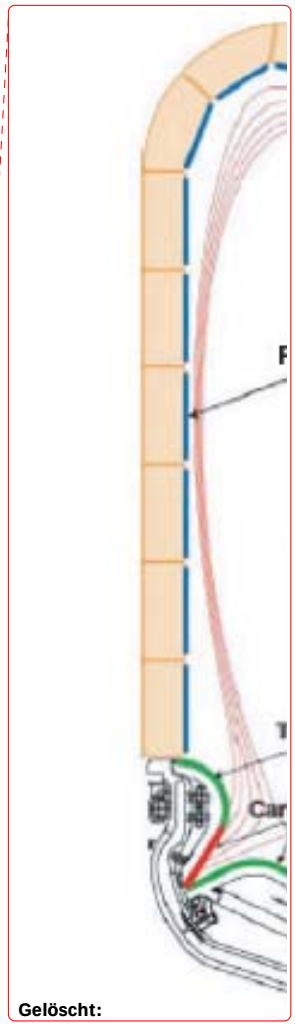

Gelöscht:

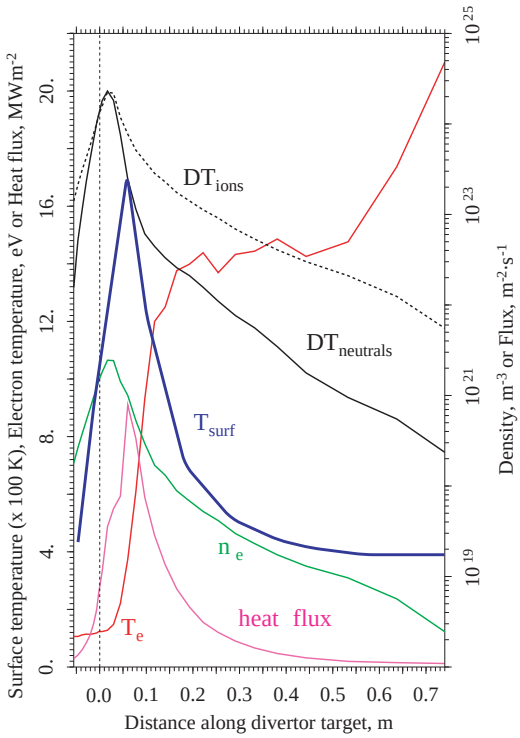

Figure 2. Plasma temperature T_e, density n_e, D/T ions and neutrals particle fluxes, heat fluxes and surface temperature along the ITER outer divertor target for a semi-detached divertor plasma for the ITER =10 reference scenario. x = 0 on the x axis corresponds to the strike point position, x < 0 corresponds to the region located below the strike point, x > 0 corresponds to the region located above the strike point.

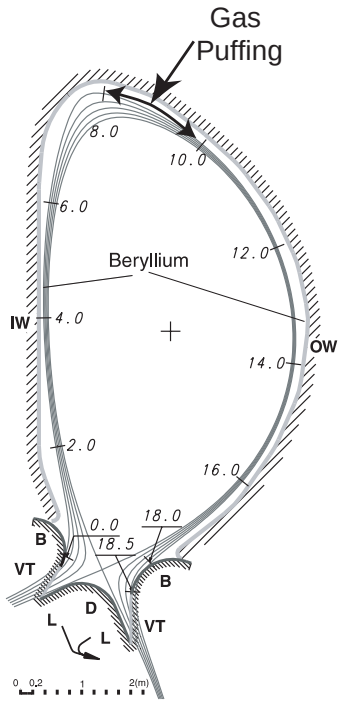

Figure 3.a. ITER poloidal cross-section showing inner (IW) and outer (OW) first wall, divertor vertical target (VT), divertor baffle (B) and divertor private region consisting of dome (D) and liner (L). Scrape-off-layer surfaces including the separatrix are shown; the numbers along the cross section give poloidal distances in meters along the separatrix, which are used in Fig. 3.b

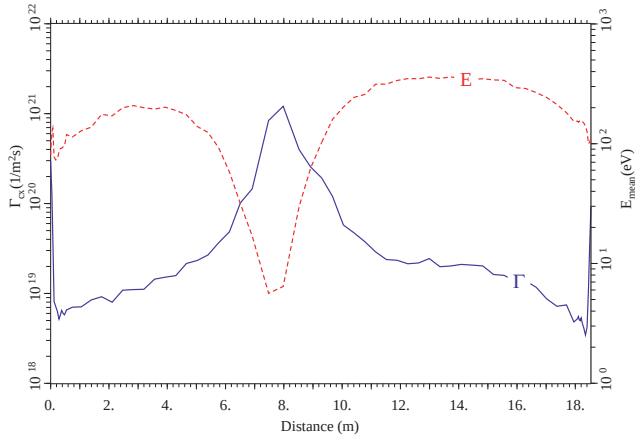

Figure 3.b. Modelled charge-exchange neutral flux and average neutral impact energy on the ITER Be first wall versus poloidal distance as defined in Fig.3.a.

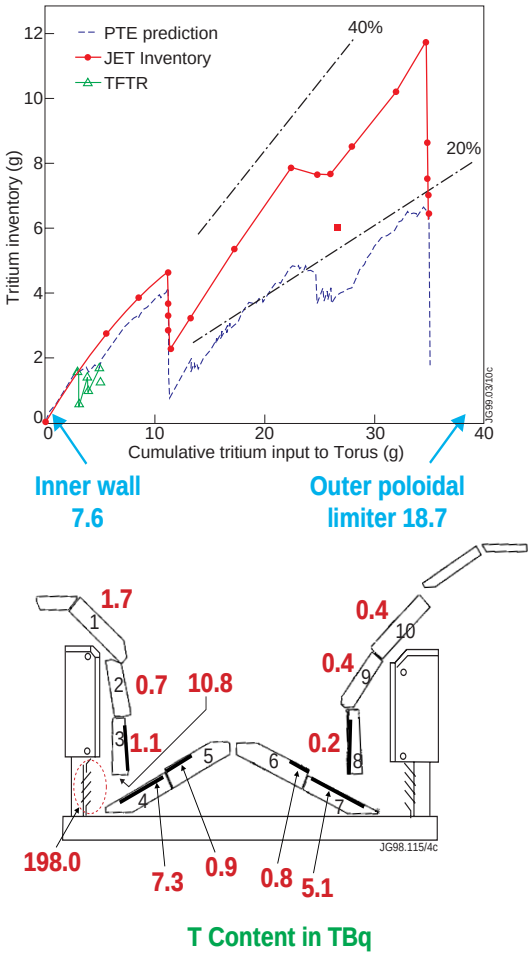

Figure 4. Upper: cumulative retention of tritium inside JET and TFTR after the tritium plasma operation campaigns [20,21]. Lower: tritium distribution in the JET tiles after cleaning procedures measured by post mortem surface analysis [24].

Gelöscht: ¶

¶

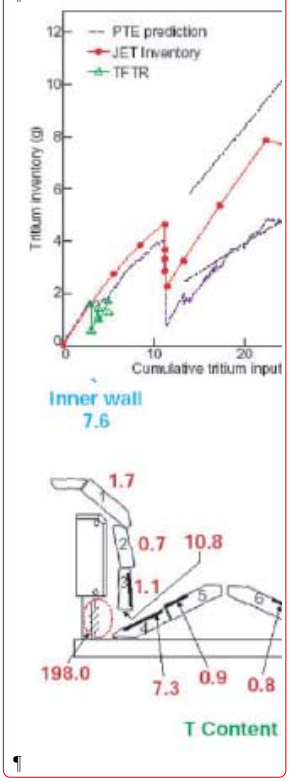

¶

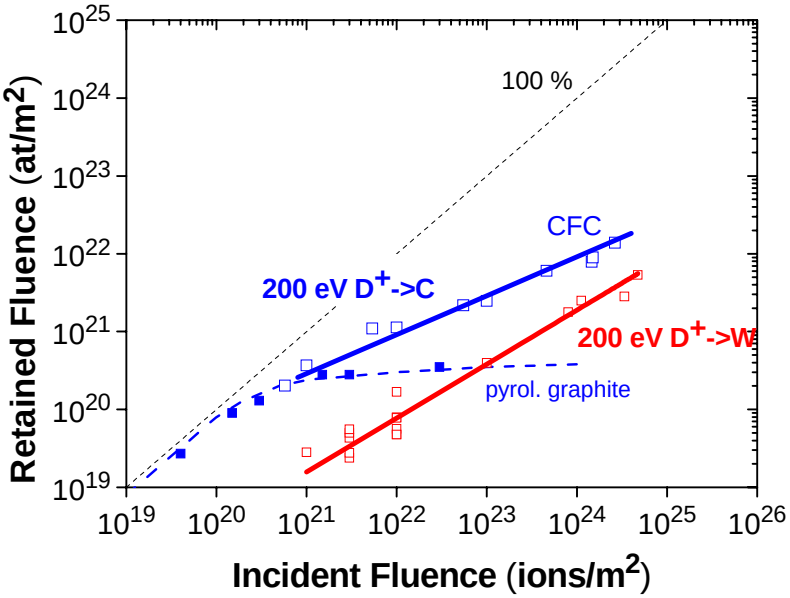

Figure 5. Retention of 200 eV D^+ deuterium in carbon (pyrolytic graphite and CFC) and polycrystalline tungsten

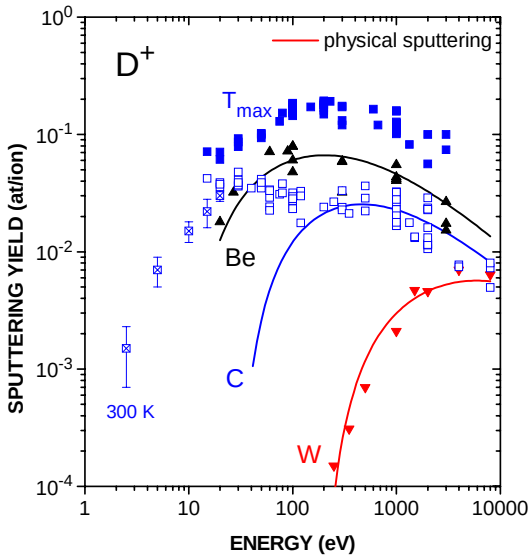

Figure 6. Sputtering yield of Be, C and W due to deuterium ions compared to an analytic description of physical sputtering.

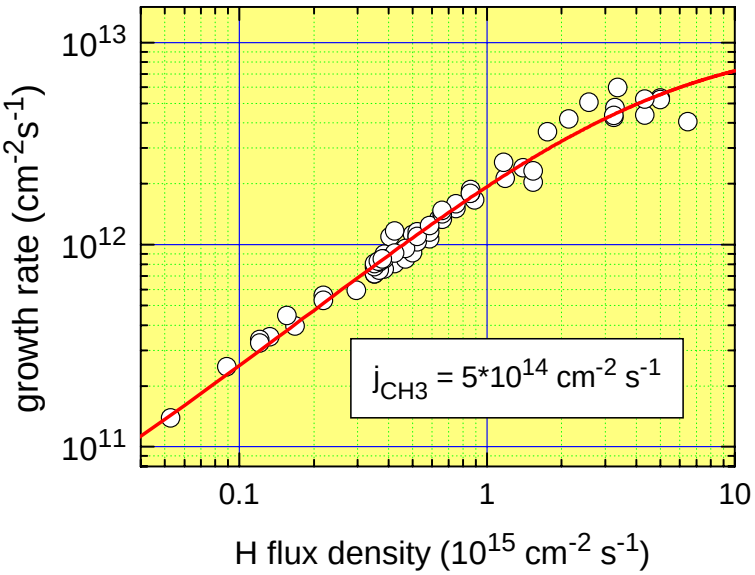

Figure 7. Growth rate of a layer on Si due to CH_3 exposure at constant flux of $5*10^{14}$ $cm^{-2}s^{-1}$ as function of simultaneous bombardment by incident hydrogen flux

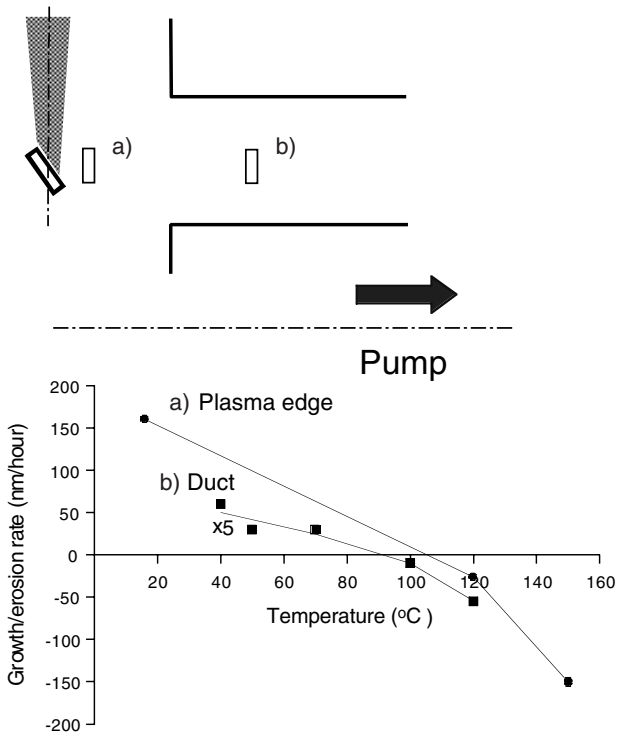

Figure 8. Balance of erosion and deposition at the plasma edge and pump duct in the PSI-2 plasma simulator versus sample temperature [65].

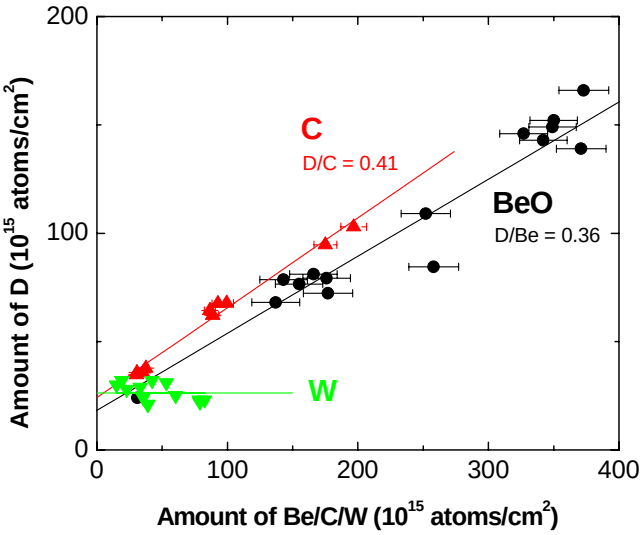

Figure 9. Co-deposited amounts of deuterium on a collector in front of different samples sputtered by 1 keV D^+ ions

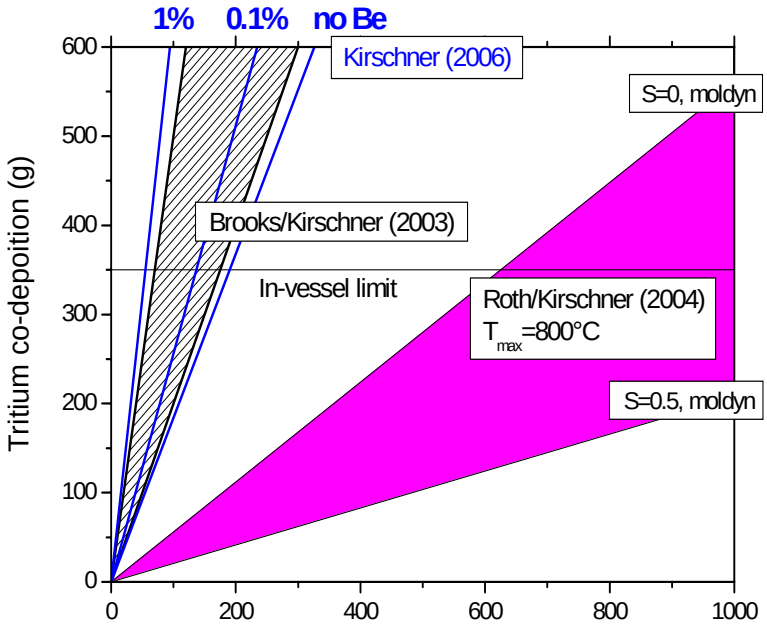

Figure 10. Estimated tritium inventory as function of the number of full, 400 s ITER D/T discharges. For details, see text.

[1] G. Federici, C.H. Skinner, J.N. Brooks, J.P. Coad, C. Grisolia, A.A. Haasz, A. Hassanein, V. Philipps, C.S. Pitcher, J. Roth, W.R. Wampler and D.G. Whyte, Nucl. Fusion **41 (**2001) 1967

[2] T. Loarer, et al. Gas Balance and Fuel Retention in Fusion Devices, IAEA Conference 2006, Chengdu, to be published

[3] Mayer, M., R. Behrisch, H. Plank, J. Roth, G. Dollinger, C.M. Frey, J. Nuclear Materials **230**, 67-73 (1996).

[4] R. Neu, R. Dux, Ch. Hopf, A. Kallenbach, Th. Pütterich, V. Rohde, A. Herrmann, K. Krieger, H. Maier, ASDEX Upgrade team: Final Steps to an All Tungsten Divertor Tokamak, J. Nucl. Materials (2006) accepted for publication

[5] Pamela, J., G.F.Matthews, V.Philipps et al., "An ITER-like Wall for JET", Proceedings of the 17th International Conference on Plasma Surface Interactions, Hefei, China (2006)

[6] Philipps, V., J. Roth and A. Loarte, Plasma Phys. Control. Fusion **45** (2003) A17

[7] Progress in the ITER Physics Basis : Chapter 4 Power and Particle Control, B. Lipschultz, A. Loarte et al. Nuclear Fusion (2006), accepted for publication

[8] ITER Technical Basis, ITER EDA Documentation Series No. 24, IAEA, Vienna 2002

[9] Merola, M., et al., J. Nucl. Mater. 307–311 (2002) 1524

[10] Loarte, A., et al., Nucl. Fusion 38 (1998) 331

[11] Kukushkin, A.S. et al., Nucl. Fusion 42 (2002) 187

[12] Federici, G., et al., J. Nucl. Mater. 313–316 (2003) 11

[13] Loarte, A., Physica Scripta T111 (2004) 13

[14] Federici, G., et al., J. Nucl. Mater. 290-293 (2001) 260

[15] Verbeek, H., Stober, J., Coster, D.P., Eckstein, W., Schneider, R., Nucl. Fusion **38** (1998) 1789.

[16] A. Kallenbach, R. Dux, J. Gafert, G. Haas, L.D. Horton, M. Jakobi, B. Kurzan, H.W. Müller, R. Neu, J. Neuhauser, R. Pugno, T. Pütterich, V. Rohde, W. Sandmann, S.-W. Yoon and the ASDEX Upgrade team, Nucl. Fusion 43 (2003) 573-578

[17] Lipschultz, B., et al., in Fusion Energy 2000 (Proc. 18th Int. Conf. Sorrento, 2000) (Vienna: IAEA) CD-ROM file EX5/6, http://www.iwww.iaea.org/programmes/ripc/physics/fec2000/html/node1.htm

[18] Rubel M et al., Phys. Scr. T **103 (**2003) 20–4

[19] Loarer T et al., 30th Conf. on Controlled Fusion and Plasma Physics (St Petersburg, Russia, 7–11 July(2003)

[20] Skinner C. et al., J. Nucl. Mater. **241–243 (**1997) 214

[21] Andrew P., Brennan P.D. and Coad J.P., Fusion Eng. Des. **47 (**1999) 233–45

[22] J. Bucalossi et al.: Deuterium in-vessel retention characterisation through the use of particle balance in Tore Supra, J. Nucl. Materials (2006) accepted for publication

[23] E. Tsitrone, Key Issues for Steady-state Operation, J. Nucl. Materials (2006) accepted for publication

[24] Coad J. P. et al., J. Nucl. **290–293 (**2001) 224

[25] Wienhold P. et al. J. Nucl. Mater. **313–316 (**2003) 311–20

[26]M. Mayer, V. Rohde, J. Likonen, E. Vainonen-Ahlgren, K. Krieger, X. Gong, J. Chen, and ASDEX Upgrade Team, J. Nucl. Materials 337-339 (2005) 119

[27] O. Gruber et al., Resent Results from ASDEX Upgrade, IAEA Conference 2006, Chengdu, to be published

[28] Roth J. and Janeschitz G., Nucl. Fusion **29 (**1989) 915

[29] Coad P. et al., J. Nucl. Mater. **313–316 (**2003) 419–23

[30] Rohde V. et a.l J. Nucl. Mater. **313–316 (**2003) 337–41

[31] Maier H. et al. J. Nucl. Mater **266–269 (**1999) 1003

[32] W.R. Wampler, C.W. Magee, J. Nucl. Materials 103&104 (1981) 509

[33] B.M.U. Scherzer, M. Wielunski, W. Möller, A. Turos and J. Roth, Nuclear Instr. & Meth. in Phys. Res. B33, (1988) 714-718

[34] R. Causey, K. Wilson, T. Venhaus, W.R. Wampler, J. Nucl. Mater. 266-269 (1999) 467

[35] W. Möller, B.M.U. Scherzer, J. Bohdansky, Retention and release of deuterium implanted into beryllium, IPP-JET Report No. 26 (1985)

[36] R.A. Anderl, R.A Causey, J.W. Davis, et al., J. Nucl. Mater. 273 (1999) 1

[37] B.L. Doyle , W.R. Wampler, D.K. Brice, S.T. Picraux, J. Nucl. Materials 93/94 (1980) 551

[38] A.A. Haasz, J. Davis, J Nucl. Mater. 209 (1994) 1140

[39] J. Roth, V.Kh. Alimov, A.V. Golubeva, R.P. Doerner, J. Hanna, E. Tsitrone, Ch. Brosset, V. Rohde, A. Herrmann, M. Mayer, J. Nucl. Materials (2006) accepted for publication

[40] R.A. Causey, T.J. Venhaus, Physica Scripta T94 (2001) 9

[41] O. Ogorodnikova, J. Roth, M. Mayer, Journal of Nuclear Materials **313-316** (2003) 469

[42] A.V. Golubeva, V.A. Kurnaev, M. Mayer, J.Roth, Int. Symp. on Hydrogen in Metals, Uppsala (June 2005) AIP to be published

[43] P. Sigmund, Phys. Rev. 184 (1969) 383

[44] J. Bohdansky, J. Roth and H.L. Bay:, J. Appl. Phys. 51 (1980) 2861

[45] J. Roth, J. Bohdansky, A.P. Martinelli, Rad. Eff. 48 (1980) 213

[46] W. Eckstein, Computer simulation of ion solid interactions, Springer Series in Materials Science (Springer Verlag, Berlin and Heidelberg, 1991), 1st ed.

[47] J. Roth, J. Bohdansky, W. Poschenrieder and M.K. Sinha, J. Nucl. Mat. 63 (1976) 222

[48] F. Meyer, this volume

[49] A. Horn A. Schenk, J. Biener, B. Winter, C. Lutterloh, M. Wittmann, J. Küppers, Chem. Phys. Lett. **231** (1994) 193

[50] U. Wenzel, M. Laux, R. Pugno, K. Schmidtmann, J. Nucl. Materials 290-293 (2001) 352

[51] E. Salonen, K. Nordlund, J. Keinonen, and C. H. Wu, Phys. Rev. B 63 (2001) 195415

[52] Roth, J., R. Preuss, W. Bohmeyer, S. Brezinsek, A. Cambe, E. Casarotto, R. Doerner, E. Gauthier, G. Federici, S. Higashijima, J. Hogan, A. Kallenbach, A. Kirschner, H. Kubo, J.M. Layet, T. Nakano, V. Philipps, A. Pospieszczyk, R. Pugno, R. Ruggiéri, B. Schweer, G. Sergienko and M. Stamp, Nuclear Fusion **44** (2004) L21

[53] D.G. Whyte, W.P. West, C.P.C. Wong, R. Bastasz, J.N. Brooks, W.R. Wampler, N.H. Brooks, J.W. Davis, R.P. Doerner, A.A. Haasz, R.C. Isler, G.L. Jackson, R.G. Macaulay-Newcombe and M.R. Wade, Nucl. Fusion **41** (2001) 1243

[54] E. Vietzke, J. Nucl. Mater. **145-147**, 443 (1987)

[55] K. Schmid, M. Baldwin, R. Doerner, J. Nucl. Materials **337-339** (2005) 862

[56] W. Jacob, C. Hopf, M. Schlüter, and T. Schwarz-Selinger, J. Nucl. Materials **337-339** (2005) 839

[57] M. Meier, A. von Keudell, J. Chem. Phys. **116** (2002) 5125

[58] W. Jacob, J. Nucl. Materials 337-339 (2005) 839

[59] D. A. Alman, D. N. Ruzic, Physica Scripta **T111** (2004) 145

[60] A. Qayyum, T. Tepnual, C. Mair, S. Matt-Leubner, P. Scheier. Z. Herman, T.D. Märk, Chem Phys. Letters 376 (2003) 539

[61] W. Schustereder, B. Rasul, N. Endstrasser, V. Grill, P. Scheier, T.D. Märk, this volume

[62] A. Kirschner, et al., Journal of Nuclear Materials **328** (2004) 62

[63] E. Vietzke, A.A. Haasz, in: W.O. Hofer, J. Roth (Eds.), Physical Processes of the Interaction of Fusion Plasmas with Solids, Academic, San Diego, 1996

Feldfunktion geändert

Feldfunktion geändert

Formatiert: Deutsch (Deutschland)

Formatiert: Deutsch (Deutschland)

[64] Bohmeyer, W., et al., Journal of Nuclear Materials **337-339** (2005) 89

[65] Bohmeyer, W., et al., Proc. 30th EPS Conf. on Controlled Fusion and Plasma Physics, St. Petersburg, Russia, 2003, Vol. 27A, p. 3.184

[66] M Mayer, V Rohde and the ASDEX Upgrade Team, Nucl. Fusion **46** (2006) 914

[67] T. Schwarz-Selinger, A. von Keudell, and W. Jacob, J Applied Physics 86 (1999) 3988

[68] W. Jacob, Thin Solid Films 326 (1998) 1

[69] M. Mayer, R. Behrisch, H. Plank, J. Roth, G. Dollinger, C.M. Frey, Journal of Nuclear Materials **230**, 67-73 (1996)

[70] M.J. Baldwin, K. Schmid, R.P. Doerner, A. Wiltner, R. Seraydarian, Ch. Linsmeier, J. Nucl. Materials 337-339 (2005) 590

[71] M. Mayer et al., Mechanism of Hydrocarbon Layer Formation in Remote Areas of Fusion Devices, EPS St. Petersburg (2003)

[72] C. Brosset et al.: Deuterium retention in gaps and deuterium inventory in deposited carbon layers in Tore Supra, J. Nucl. Materials (2006) accepted for publication

[73] T. Nakano, N. Asakura, H. Takenaga, H. Kubo,K. Shimizu, H. Kawashima and the JT-60 Team: Particle control under wall saturation in long-pulse discharges in JT-60U, J. Nucl. Materials (2006) accepted for publication

[74] J. Brooks, A. Kirschner, J. Nucl. Mater. 313-316 (2003) 424

[75] J. Roth, A. Kirschner et al. J. Nucl. Mater. **337-339** (2005) 970

[76] A. Kirschner, D. Borodin, S. Droste, V. Philipps, U. Samm, G. Federici, A. Kukushkin, A. Loarte: Modelling of tritium retention and target lifetime of the ITER divertor using the ERO code, J. Nucl. Materials (2006) accepted for publication

[77] A. Kirschner, V. Philipps, J. Winter, U. Kögler, Nuclear Fusion 40 (2000) 989.